Published in final edited form as:
Mech Dev. 2011 September ; 128(7-10): 442–456. doi:10.1016/j.mod.2011.08.004.

The role of *stat1b* in zebrafish hematopoiesis

Hao Song, **Yi-lin Yan**, **Tom Titus**, **Xinjun He**, and **John H. Postlethwait**
Institute of Neuroscience, University of Oregon, OR 97403 USA

Hao Song: hsong@uoregon.edu; Yi-lin Yan: yan@uoneuro.uoregon.edu; Tom Titus: titus@uoneuro.uoregon.edu; Xinjun He: xhe@uoneuro.uoregon.edu; John H. Postlethwait: jpostle@uoneuro.uoregon.edu

Abstract

STAT1 mediates response to interferons and regulates immunity, cell proliferation, apoptosis, and sensitivity of Fanconi Anemia cells to apoptosis after interferon signaling; the roles of STAT1 in embryos, however, are not understood. To explore embryonic functions of STAT1, we investigated *stat1b*, an unstudied zebrafish co-ortholog of human *STAT1*. Zebrafish *stat1a* encodes all five domains of the human STAT1-alpha splice form but, like the human STAT1-beta splice variant, *stat1b* lacks a complete transactivation domain; thus, two unlinked zebrafish paralogs encode protein forms translated from two splice variants of a single human gene, as expected by subfunctionalization after genome duplication. Phylogenetic and conserved synteny studies showed that *stat1b* and *stat1a* arose as duplicates in the teleost genome duplication (TGD) and clarified the evolutionary origin of *STAT1*, *STAT2*, *STAT3*, *STAT4*, *STAT5A*, *STAT5B* and *STAT6* by tandem and genome duplication. RT-PCR revealed maternal expression of *stat1a* and *stat1b*. *In situ* hybridization detected *stat1b* but not *stat1a* expression in embryonic hematopoietic tissues. Morpholino knockdown of *stat1b*, but not *stat1a*, decreased expression of the myeloid and granulocyte markers *spi* and *mpo* and increased expression of the hematopoietic progenitor marker *scl*, the erythrocyte marker *gata1*, and hemoglobin. These results suggest that zebrafish Stat1b promotes myeloid development at the expense of erythroid development.

Keywords

Stat1α; Stat1β; hematopoiesis; myeloid; granulocyte; zebrafish; genome duplication; subfunctionalization; Fanconi anemia

1. Introduction

Blood cell lineages arise by lineage commitment and cell maturation. The helix-loop-helix transcription factor SCL/TAL1 causes hemangioblasts to become hematopoietic stem cells (HSC) and mice lacking *SCL* activity fail in embryonic erythropoiesis (Forrai and Robb, 2003; Shivdasani et al., 1995; Xiong, 2008). HSCs develop into erythroid, myeloid, and lymphoid lineages marked by lineage-specific transcription factors, including GATA1 for erythroid differentiation (Crispino, 2005; Fujiwara et al., 1996), SPI1 (PU.1) for the myeloid lineage (Kastner and Chan, 2008; Oikawa et al., 1999), and IKAROS for lymphoid

Corresponding author: John H. Postlethwait: Professor of Biology, 1254 University of Oregon, 1425 E. 13th Avenue, Eugene OR 97403 USA; Phone: (541) 346-4538; jpostle@uoneuro.uoregon.edu.

differentiation (Georgopoulos et al., 1997; Schmitt et al., 2002). Although much is known, we lack details concerning the networks of factors that regulate these cell fate-marking genes.

Proinflammatory cytokines, such as IFN-gamma, can impact hematopoietic development (Baldridge et al., 2010). IFN-gamma binds its receptor, thus activating JAK proteins, which phosphorylate STAT (signal transducer and activator of transcription) proteins that then translocate to the nucleus where they bind DNA and activate expression of IFN-stimulated genes (Schindler et al., 1992; Stark et al., 1998). IFN-gamma, for example, promotes the proliferation of repopulating HSCs and this response requires STAT1 (Baldridge et al., 2010; Zhao et al., 2010). Furthermore, about half of AML (acute myeloid leukemia) patients have constitutive STAT1 activity (Aronica et al., 1996; Gouilleux-Gruart et al., 1997; Weber-Nordt et al., 1996). Mammals have seven STAT genes (STAT1, STAT2, STAT3, STAT4, STAT5A, STAT5B, and STAT6) but their historical origins have not yet been fully explained.

STAT1 transduces signals in response to a variety of cytokines and growth factors (Najjar et al., 2010; Najjar and Fagard, 2010) and regulates a number of cellular functions, mainly in the immune system. In addition to type I and type II IFNs, which use STAT1 to fight against opportunistic virus infections (Durbin et al., 1996; Meraz et al., 1996), growth factors including EGF (Chin et al., 1996) and PDGF (Vignais et al., 1996) can activate STAT1. Moreover, STAT1 is activated by numerous interleukins (ILs) that regulate growth of various white blood cells (Najjar and Fagard, 2010). cytokines [69]. In mouse and human, Fanconi Anemia mutant hematopoietic progenitor cells are hypersensitive to IFN signaling due to increased apoptosis, and this is mediated by STAT signaling (Haneline et al., 1998; Li et al., 2004; Otsuki et al., 1999; Pang et al., 2000; Rathbun et al., 1997; Si et al., 2006; Whitney et al., 1996; Zhang et al., 2004).

Human *STAT1* produces two splice variants that differ at their carboxy terminus. STAT1-alpha contains a TAZ2-binding, trans-activation domain (TAD) that is missing from the shorter, STAT1-beta isoform, which acts as a dominant negative regulator of STAT1 function (Bromberg et al., 1996). STAT1-beta inhibits the apoptotic effect of STAT1-alpha in B lymphocytes (Baran-Marszak et al., 2004) but induces cell death in B-cells by a p53-independent mechanism (Najjar et al., 2008). Other functions of these two splice forms have yet to be identified.

Zebrafish provides a good model for the investigation of the conserved functions of STAT1 and vertebrate hematopoiesis (Bertrand and Traver, 2009; Ciau-Uitz et al., 2010; Ellett and Lieschke, 2010; Paik and Zon, 2010). Transcriptional mechanisms of both primitive (embryonic) and definitive (adult) hematopoiesis are evolutionarily conserved among vertebrates but the anatomical location varies among species (de Jong and Zon, 2005). In zebrafish, primitive hematopoiesis begins at 10 hours post-fertilization (hpf) when the ventral lateral plate mesoderm gives rise to embryonic HSCs, which occupy the intermediate cell mass (ICM) and differentiate mainly into pro-erythroblasts, and the rostral blood island (RBI), which produces mostly macrophages (Davidson et al., 2003; Long et al., 1997). At 24 hpf, about 300 erythrocytes enter the blood stream from the ICM (Patterson et al., 2005), and several hours later, definitive HSCs begin to appear in the ventral wall of the dorsal aorta (the aorta-gonad-mesonephros, AGM) (Burns et al., 2005). Hematopoiesis continues in the AGM until a few hours before hatching, when the kidney marrow initiates lifelong definitive hematopoiesis (Traver, 2004)).

While STAT1 functions have been well studied in mammalian tissue culture cells, comparatively little work has been directed toward the roles of STAT1 in intact developing

vertebrate embryos. Zebrafish has several advantages for the investigation of STAT1 in living embryos. First, as in mammals, zebrafish responds to LPS (the bacterial cell wall component lipopolysaccharide) by increased expression of IL1 and TNF (tumor necrosis factor) (Sullivan et al., 2009). Second, zebrafish *stat1a* can rescue interferon signaling-mediated cell growth inhibition in a STAT1-deficient human cell line (Oates et al., 1999b). Third, zebrafish conserves a role of *jak2a* in hematopoiesis (Oates et al., 1999a), raising the hypothesis that it may act upstream of zebrafish *stat1*. Fourth, due to the teleost genome duplication (TGD) at the base of the teleost radiation, many single copy genes in human have two orthologs in zebrafish (Amores et al., 1998; Amores et al., 2004; Jaillon et al., 2004; Postlethwait et al., 1998; Taylor et al., 2003). Such duplicates often share between them ancestral gene functions that are conserved in a single orthologous gene in mammals (Force et al., 1999; Postlethwait et al., 2004). Thus, knockdown of just one of the two duplicates can reveal gene functions that might be difficult to identify in mammals due to pleiotropy. We capitalized on this approach to investigate the functions of two zebrafish *STAT1* co-orthologs and thereby provide new insights into the roles of STAT1 in hematopoietic development. Here we show that *stat1b* arose in the teleost genome duplication event, that it is expressed in the embryonic hematopoietic compartment, and that it promotes development of the myeloid lineage at the expense of the erythroid lineage.

2. Results

2.1. Zebrafish has two genes related to human *STAT1*

Because about a quarter of human genes have two co-orthologs in zebrafish due to the teleost genome duplication (Postlethwait et al., 1998), we searched for a zebrafish duplicate of the previously described *stat1a* gene (Oates et al., 1999b). A BLAST search (Altschul and Koonin, 1998) of *stat1a* (GenBank: **M97936**) against the zebrafish EST database identified EST RK103A3G02.T3 (GenBank: **CD596714**), which was isolated from adult zebrafish kidneys, the site of definitive hematopoiesis (Song et al., 2004), and had just 78% identity at the amino acid level with *stat1a*; this low level of identity suggested that these ESTs were from two different genes. A search of CD596714 against the *Ensembl* zebrafish genome hit a genomic sequence (ENSDARG00000076182, GenBank: **XR_029517**) that we now call *stat1b*. We designed primers to amplify overlapping fragments of the gene model and used them to amplify gene fragments from cDNA extracted from 24 – 48 hpf wild-type zebrafish embryos. We sequenced these fragments and assembled them to reconstruct the sequence of a complete cDNA (GenBank: **FJ986224**).

Comparing the structure of our 3,569 bp-long *stat1b* cDNA with genomic DNA at *Ensembl* revealed 23 exons. Both zebrafish *stat1* genes appeared to lack the first of two untranslated exons in human *STAT1* (Fig. 1A), consistent either with the loss of the first untranslated exon in the zebrafish lineage or the gain of this exon in the human lineage. A BLASTX search of the human genome with either our new *stat1b* gene or the previously known *stat1a* gene returned *STAT1* as the most similar human gene, and reciprocally, a BLASTP search of zebrafish sequences with the human STAT1 protein hit zebrafish Stat1a and Stat1b as the two most similar sequences, as would be expected if *stat1a* and *stat1b* were co-orthologs of *STAT1*.

2.2. Conserved domains in zebrafish Stat1 proteins

The protein predicted from our *stat1b* cDNA sequence contains 725 amino acids (GenBank: **ACR83062**). The Conserved Domain Database (Marchler-Bauer et al., 2009) showed that the translated Stat1b peptide has all but one of the five domains that are required for STAT function (Brierley and Fish, 2005). Conserved domains (Fig. 1B) include (1) the N-terminal 130 amino acids that constitute the STAT dimer *interaction* stabilization domain

(STAT_int) (Vinkemeier et al., 1998); (2) a *coiled-coil* domain (STAT_alpha, at about residues 135 – 315) that contains four alpha helices with hydrophilic surfaces that mediate interactions with non-STAT1 alpha-helical proteins (Becker et al., 1998); (3) the *DNA binding domain* (DBD or STAT_bind, at about residues 320 – 480) consisting of a beta-barrel that determines DNA binding specificity (Chen et al., 1998); (4) the phosphotyrosine-binding *SH2* domain (SH2, at about residues 580–680) that recognizes phosphorylated tyrosine motifs in cytokine receptors, JAKs, and other STAT proteins (Kisseleva et al., 2002). Stat1b, however, lacks (5) the C-terminal *trans-activation domain* (TAD or STAT1_TAZ2bind, at about residues 723–747 in zebrafish Stat1a) that binds TAZ2 domains and mediates interactions with cofactors that facilitate transcriptional activation (Decker and Kovarik, 2000) (Fig. 1B and Supplementary Fig. S1). This domain analysis showed that zebrafish Stat1b has the domain structure of the human STAT1-beta splice variant and that zebrafish Stat1a has the domain structure of the human STAT1-alpha splice variant. This domain distribution would be expected if the ancestral STAT1 protein had all five domains and that in the zebrafish lineage, the TAZ2bind domain was preserved by the *stat1a* gene but was lost by the *stat1b* gene, while in the human lineage, the TAZ2bind domain was preserved by the single STAT1 gene and that differential splicing provides the two isoforms, one with and one without the TAZ2bind domain; thus, two different molecular genetic mechanisms provide a pair of structurally similar isoforms in zebrafish and human.

2.3. Functional amino acid residues in Stat1b

Protein alignments showed that zebrafish Stat1b and Stat1a proteins generally conserve amino acids required for STAT1 function (Brierley and Fish, 2005) (Supplementary Fig. S1). In human STAT1, an arginine at position 31 becomes methylated (Mowen et al., 2001), and this site is conserved in zebrafish Stat1a and Stat1b proteins. The human DBD requires K366, V426, and T427, which correspond to K372, V432, and T433 in zebrafish Stat1b, and these residues are also conserved in Stat1a. Crystal structure of human STAT1 shows that H431, R378, and V457 are in positions critical for DNA binding (Chen et al., 1998), and these are all conserved in both zebrafish Stat1a and Stat1b proteins. Although STAT1 bound to DNA shows N460 located in the major groove, its mutation did not block IFN-gamma-induced binding of STAT1 to DNA (Yang et al., 2002) and, correspondingly, this residue is conserved in Stat1a but not Stat1b. R602 and P633, which are required for activity of the SH2 domain (Brierley and Fish, 2005; Improta et al., 1994), are conserved in both Stat1b and Stat1a. In the C-terminal region, the phosphorylation site Y701 in the human STAT1 protein is conserved in zebrafish Stat1a but not in Stat1b (Supplementary Fig. S1). Finally, the phosphorylated serine S727 in the TAZ2bind transactivation domain of human STAT1alpha is conserved in Stat1a and a serine is also present in a similar position in Stat1b despite its greatly disrupted TAZ2bind domain. We conclude that both zebrafish Stat1 proteins generally conserve protein domains shown to be functional in human STAT1, except for the C-terminal transactivation domain that is greatly disturbed in zebrafish Stat1b and the human STAT1beta splice form.

2.4. Zebrafish *STAT1* co-orthologs originated in the teleost genome duplication

To help understand the origin of *stat1b*, we conducted a phylogenetic analysis of full-length STAT proteins using maximum likelihood (Guindon and Gascuel, 2003). The seven human STAT proteins occupied six well-supported clades (Fig. 2). The zebrafish Stat1b protein fell snugly into the STAT1 clade with good bootstrap support. The sister clade to zebrafish *stat1b* was represented by a highly similar sequence in goldfish, which is a cyprinid like zebrafish. Stickleback, a percomorph fish, contained a rapidly evolving sequence related to *stat1b*, although other sequenced percomorphs, including medaka and two pufferfish, appeared to lack a *stat1b* ortholog. The *stat1b* clade branched as a sister to the *stat1a* clade,

which included sequences from several percomorphs. This tree morphology is predicted by the hypothesis that *stat1a* and *stat1b* arose in a gene duplication event after the divergence of ray-fin and lobe-fin fish but before the teleost radiation, a situation consistent with the hypothesis that these two paralogs arose in the teleost genome duplication event.

To confirm the affinities of the *stat1b* clade (78% bootstrap support), we explored conserved syntenies around *stat1b* using the Synteny Database (Catchen et al., 2009) and the zebrafish genome at Ensembl. The hypothesis that *stat1a* and *stat1b* arose in the TGD predicts that zebrafish should have two chromosomal segments co-orthologous with the region on human chromosome 2 (Hsa2) surrounding *STAT1*. Figure 3 shows that orthologs of genes surrounding *STAT1* (Fig. 3B) appear in two locations in the zebrafish genome, one on *Danio rerio* linkage group 9 (Dre9, Fig. 3A) and the other on Dre22 (Fig. 3C). *STAT1* lies adjacent to *STAT4* on Hsa2 and the two genes are transcribed in the same direction. Likewise, on Dre9, *stat1b* resides next to *stat4* in the same orientation. Except for an inversion, the human orthologs of an additional 15 genes surrounding *stat1b* are located in the same order and direction surrounding *STAT1* on Hsa2 (compare Fig. 3A and 3B). Zebrafish *stat1a* lies on Dre22 near ten other genes whose human orthologs are located near *STAT1*. This double syntenic conservation, coupled with the phylogenetic analysis showing that *stat1b* and *stat1a* occupy sister clades, strongly supports the conclusion that *stat1b* and *stat1a* arose in the TGD. Furthermore, the conserved synteny of eight of eleven genes in a row (including *stat4*) in the stickleback and zebrafish genomes confirms the orthology of *stat1b* in these two species despite the rapid evolution of the stickleback gene (Supplemental Fig. S3).

The second copy of *stat4* that would have been produced by the TGD and should lie next to *stat1a* appears to be missing from the zebrafish genome. Relative to Dre9 and the human *STAT1* region, an inversion breakpoint is in the location expected for the duplicate copy of *stat4* on Dre22, suggesting that a chromosome break occurred in this location after the TGD. This break could have initiated the destruction of this *stat4* copy. The loss of the *stat4* duplicate on the ancestral chromosome segment of Dre22 would be expected to have had no phenotypic penalty if its functions were fully redundant with the *stat4* copy retained on Dre9. Because gene orientation in both zebrafish Dre9 and human Hsa2 is 5′-*stat4*-*stat1*–3′, an inversion between the genes could have disrupted *cis*-acting regulatory elements located in the intergenic region, thus resulting in the loss of ancestral regulatory elements originally associated with the ancestral *stat1a* and its originally adjacent *stat4* gene.

2.5. History of the vertebrate *STAT* gene family

Phylogenetic and conserved synteny analysis help infer the origins of the entire STAT family. In a maximum likelihood tree, the seven human *STAT* genes (*STAT1, 2, 3, 4, 5A, 5B,* and *6*) fell into six well-supported clades reflected by their names (Fig. 2). Two *stat* genes from the sea squirt *Ciona intestinalis*, a Urochordate representing the sister group to the vertebrates, and a *stat*-related gene from fruit fly fell in the phylogeny unexpectedly in the *STAT5* and *STAT6* clades rather than as outgroups. These locations may be artifacts due to the long branches of these taxa. The six vertebrate *STAT* clades further subdivided into two strongly supported subclades, one containing *STAT1, 2, 3,* and *4*, and the other containing *STAT5* and *6* (Fig. 2). This evidence suggests that an ancestral *STAT* gene experienced an early gene duplication event that produced a *STAT1234* gene and a *STAT56* gene (Fig. 4A, B). Because the seven human *STAT* genes occur in three gene clusters (Fig. 3E–F), this ancient event was probably a tandem duplication. Use of the Synteny Database (Catchen et al., 2009) showed that the three *STAT* clusters appear on Hsa2 (*STAT1* and *STAT4*), Hsa12 (*STAT2* and *STAT6*), and Hsa17 (*STAT3*, *STAT5A*, and *STAT5B*) in genome neighborhoods that contain many paralogous genes, including three *HOX* clusters (*HOXD, HOXC,* and *HOXB*, respectively). These genome neighborhoods, along with the *HOXA* region on Hsa7, which lacks any *STAT* family genes, arose in two rounds of whole genome duplication at the

base of the vertebrate radiation (Dehal and Boore, 2005; Holland et al., 1994; Ohno, 1970) (Fig. 4C, D). *STAT4* and *STAT1* are adjacent and transcribed in the same direction in human and *stat4* and *stat1b* in zebrafish share this genomic arrangement (Fig. 4F). The fact that the *STAT1* and *STAT4* clades are both in the *STAT1234* clade with strong bootstrap support and are sister groups (although with low bootstrap support, Fig. 2) suggests that *STAT1* and *STAT4* arose by tandem duplication after the second round of vertebrate genome duplication R2 and that this chromosome's *STAT56* paralog was lost (Fig. 4E). Because *STAT2* and *STAT6* are spaced 18 genes apart in the GRCCh37 version of the human genome and are transcribed in opposite orientations with respect to *stat3* and *stat5.1* in zebrafish, inversions must have separated them after the R2 event (Fig. 4D, E). After the divergence of the zebrafish and human lineages (Fig. 4E, F), the TGD event would have duplicated the ancestral gene content in the zebrafish lineage. After the TGD, gene loss continued, as duplicate copies of *stat4, stat2, stat6, and stat3* were lost (Fig. 4F). Finally, after the human lineage diverged from the chicken lineage, a tandem duplication event produced *STAT5A* and *STAT5B* (Fig. 4F). Note that *stat5.1* and *stat5.2* in zebrafish are both co-orthologous to both *STAT5A* and *STAT5B* in human due to independent duplications in each lineage (Lewis and Ward, 2004).

2.6. *stat1a* and *stat1b* are both expressed in early zebrafish development

Having established the historical relationships of the vertebrate *STAT* gene family, we turned to the investigation of *stat1* functions. First, we followed the developmental time course of *stat1a* and *stat1b* expression by RT-PCR using total RNA samples from zebrafish embryos of various ages. To calibrate this semi-quantitative technique, we made a dilution series of the RNA template and amplified with *stat1a* or *stat1b* primers or with actin primers for loading control and amplified for just 21 cycles of PCR to avoid saturation. Results showed that under these conditions, band intensity depended on template concentration (Fig. 5A). Use of the same conditions on embryo RNAs revealed strong and steady expression of *stat1a* from 0.5 hpf (two-cell stage) until 96 hpf (= 2 day post hatching) (Fig. 5B). We conclude that *stat1a* is expressed maternally followed by persistence of the transcript and that the zygotic *stat1a* gene is expressed later, verifying previous results (Oates et al., 1999b). For *stat1b*, transcript levels were low in two-cell embryos (0.5hpf) and then disappeared during cleavage (2 hpf); but then by 5 hpf, about two hours after the mid-blastula transition when transcription commences from zygotic genes (Kane and Kimmel, 1993), quantities of *stat1b* mRNA began to rise, dipped somewhat after 24 hpf, and then rose again at 96 hpf. We conclude that *stat1a* is expressed maternally and that both *stat1a* and *stat1b* are expressed zygotically through embryogenesis.

2.7. Hematopoietic tissues express *stat1b*

To verify the RT-PCR experiments and to learn which tissues express *stat1* transcripts, we explored gene expression by whole mount in situ hybridization. In situ hybridization experiments revealed that *stat1a* is expressed ubiquitously at a low level throughout the embryo (data not shown), confirming the previous report (Oates et al., 1999b). In contrast to *stat1a*, *stat1b* showed strong and restricted expression by in situ hybridization. Beginning at the 2-somite stage (about 11 hpf), signal for *stat1b* appeared strongly and specifically in bilateral stripes in the lateral plate mesoderm (Fig. 6A–D). These stripes eventually migrated medially and fused to form the intermediate cell mass (ICM) by the 18-somite stage (17hpf, Fig. 6E, F). This pattern is similar to that shown by *gata1*, where at 16 hpf, *gata1*-expressing cells mark stripes of erythroid progenitors (de Jong and Zon, 2005). At 24 hpf, *stat1b* expression appeared in the ICM (Fig. 6G), the location of erythropoiesis at this stage (de Jong and Zon, 2005). Later, at 32 hpf and 48 hpf, *stat1b* expression broke up into islands in the ventral vasculature and advanced to the heart and the ducts of Cuvier, which form after 25 hpf and contain both erythrocytes and myeloid cells (Fig. 6H, I). The expression pattern

of *stat1b* mimics those of hematopoietic marker genes, including *gata1*, *gata2* and *hbbe* (Detrich et al., 1995).

2.8. *stat1b* functions in hematopoietic cell lineage specification

The early and specific expression of *stat1b* in the ICM suggested that *stat1b* might play a role in primitive hematopoietic development. To test this hypothesis, we knocked down activity of *stat1a* and *stat1b* in developing zebrafish embryos by injecting early cleavage embryos with either *stat1a* or *stat1b* antisense morpholino oligonucleotide (MO) directed against intron/exon borders and then queried various blood cell lineages by investigating the expression of lineage-specific gene markers. We first verified the efficacy of the splice-inhibiting MOs by RT-PCR of cDNA extracted from 24–48 hpf embryos that were injected with MO at the 1–2 cell stage. Results showed that the *stat1a* and *stat1b* MOs were both effective inhibitors of transcript splicing (Supplementary Fig. S2). Translation of the unspliced transcript into intron-3 of *stat1a* predicted a premature in-frame stop codon at 127 residues of the 749 amino acid protein and translation reading into intron-5 of *stat1b* predicted a premature stop codon at 201 amino acids of the full length 725 residue protein.

To test whether *stat1b* plays a role in the development of hematopoietic stem cells (HSC), we investigated expression of *scl* (*tal1*) (Liao et al., 1998) in *stat1a* and *stat1b* knockdown animals. Results showed that 16 hpf and 32 hpf embryos injected with *stat1a* MO showed the same expression compartment of *scl* as those injected with control MO (Fig. 7A, B). In contrast, 16 hpf and 32 hpf embryos injected with *stat1b* MO contained a substantially broader band of *scl* expression than control-MO injected animals (Fig. 7C). To quantitate levels of *scl* expression, we performed quantitative PCR on RNA extracted from control and treated embryos. Results confirmed that knockdown of *stat1a* had no effect *on scl* transcript levels, but that *stat1b* knockdown resulted in significantly higher levels of *scl* expression than in controls, although the effect had diminished by 32 hpf (Fig. 7G). We conclude that *stat1b*, but not *stat1a*, normally limits the width of the striped compartment of *scl*-expressing hematopoietic progenitor cells and the amount of *scl* expression in 16 hpf embryos.

After the specification of hematopoietic stem cells, the primitive erythroid lineage expresses *gata1* (Detrich et al., 1995). Knockdown of *stat1a* had little effect on *gata1* expression at 16 hpf or 32 hpf (Fig. 7H, I, K, L), but knockdown of *stat1b* activity resulted in broader and denser *gata1* expression compartments at both stages (Fig. 7J, M). Q-PCR experiments confirmed these results (Fig. 7N). These experiments suggest that *stat1b* normally suppresses the extent of the *gata1* expression compartment. If *stat1b* activity inhibits the formation of *gata1* expressing cells, then it should affect erythrocyte development. To test whether *stat1b* activity is involved in the development of hemoglobin-producing cells, we stained control and *stat1b* knockdown individuals at 2dpf with *o*-dianisidiine, a stain for hemoglobin. Results showed a substantial increase in hemoglobin-producing cells after *stat1b* knockdown relative to uninjected controls, control MO injected animals, and *stat1a* treated embryos (Supplementary Figure s4). We conclude that *stat1b* activity inhibits erythrocyte development.

To investigate the role of *stat1b* on myeloid cell development, we studied *spi1* (*pu.1*) (Lieschke et al., 2002) and to assay heterophil granulocytes, we used myeloperoxidase (*mpo*) (Bennett et al., 2001). Both markers were depressed after knockdown of *stat1b* in both RNA *in situ* hybridization assays and in Q-PCR assays, while *stat1a* knockdown had no effect (Fig. 7). The decrease in expression of myeloid cells and granulocytes after *stat1b* knockdown shows that Stat1b normally promotes myeloid cell development. Markers for definitive HSC, macrophages, and lymphoid cells – as marked by *c-myb* and *runx1*, *l-plastin*, and *rag1*, respectively (Herbomel et al., 1999; Kalev-Zylinska et al., 2002; Thompson et al., 1998; Willett et al., 1997) -- showed no expression differences between

control animals and embryos injected with either *stat1a* or *stat1b* MOs (data not shown). To test whether cell death plays a prominent role in the effect of *stat1b* knockdown, we stained uninjected controls, and animals injected with control-MO, *stat1a* MO, or *stat1b* MO with acridine orange, which stains apoptotic cells, and then counted stained cells after spinning disc confocal microscopy. Results showed no differences among treatment groups (data not shown), suggesting that cell death does not play a large role in *stat1b*-mediated effects. Taken together, these analyses show that the knockdown of *stat1b* results in an expansion of the erythroid territory and a depression of the myeloid territory, while other hematopoietic lineages remain intact.

3. Discussion

Experiments reported here cloned *stat1b* cDNA, showed that its sequence is similar to that of the human *S*TAT1beta splice form, defined *stat1b* history in the context of the evolution of the full vertebrate *STAT* family through tandem duplication and three rounds of whole genome duplication, identified *stat1b* expression in primitive hematopoietic cells, and showed that *stat1b* functions to promote the myeloid lineage at the expense of the erythroid lineage.

Mice lacking both STAT1alpha and STAT1beta develop normally but do not respond normally to interferons (Durbin et al., 1996; Meraz et al., 1996). In mammals, STAT1alpha contains a C-terminal transcription activation domain and is a fully functional transcriptional activator, while STAT1beta is a splice variant that lacks the TAD and fails to stimulate transcription in vitro from a chromatin template (although it can stimulate transcription from naked DNA) (Schindler et al., 1992; Zakharova et al., 2003). In a human lymphoblastoid cell line, forced expression of STAT1beta inhibited the phosphorylation, DNA-binding activity, and transcription activating function of STAT1alpha, and the expression of STAT1alpha target genes, while also increasing cell proliferation and resistance to fludarabine-induced cell cycle arrest and apoptosis, suggesting that STAT1beta is a dominant negative regulator of STAT1alpha (Baran-Marszak et al., 2004; Bromberg et al., 1996; Muller et al., 1993). Expression of a STAT1 form that, like STAT1beta, lacks critical features of transcription activating domain acts as a dominant negative inhibitor of STAT1 action (Bromberg et al., 1998).

Comparative analysis showed that, like human STAT1beta, zebrafish Stat1b protein lacks a complete TAD, but zebrafish Stat1a maintains a full C-terminal TAD like human STAT1alpha. Thus, zebrafish Stat1b has a structure homologous to the human dominant negative form, suggesting that Stat1b may act in zebrafish as a dominant regulator of Stat1a. Because the zebrafish Stat1a protein rescues interferon-signaling in a STAT1-deficient human cell line (Oates et al., 1999b), the zebrafish and human Stat1 systems appear to conserve basic mechanisms in cytokine signaling.

This raises the hypothesis that some of the STAT functions that partition between splice forms in mammals divide between duplicated genes in zebrafish. This type of subfunctionalization of protein functional domains is predicted by the duplication-degeneration-complementation hypothesis (Force et al., 1999; Postlethwait et al., 2004).

For vertebrate genes in the STAT3, STAT4, and STAT5 clades, teleosts and tetrapods have evolutionary rates (branch lengths on the phylogenetic tree) that are approximately equivalent, whether they are duplicated (like *stat5.1* and *stat5.2*) or not (like *stat3* and *stat4*). In contrast, in the STAT1 clade, teleost genes are evolving more rapidly than their tetrapod orthologs: *stat1b* is evolving especially rapidly in stickleback and appears to have been lost by other sequenced perciform fish. The sharing of functions between gene duplicates is

thought to relax pleiotropy and thus may provide opportunities to contribute to more rapid protein sequence evolution in some situations. In contrast to the STAT3, 4, and 5 clades, the STAT2 and 6 clades are rapidly evolving in both in tetrapods and in teleosts. Curiously, *STAT2* and *STAT6* genes appear to have experienced an inversion event that separated these paralogs, which initially arose from a tandem duplication event, with 20 genes between them now in the human genome. By inserting break points in intergenic regions, this inversion may have altered gene regulation and expression compartments in ways that relaxed selection on the protein-coding regions of *STAT2* and *STAT6* genes.

Functionally, zebrafish *stat1a* and *stat1b* genes differ in several key respects. First, *stat1b* is expressed early and strongly in hematopoietic tissues in zebrafish embryos, while in situ hybridization studies showed that *stat1a* is expressed at low levels ubiquitously, confirming previous results (Oates et al., 1999b). These findings are consistent with our RT-PCR studies on whole embryos that revealed transcript for both *stat1a* and *stat1b* in embryos. According to the duplication-degeneration-complementation hypothesis, the partitioning of ancestral subfunctions, including tissue-specific regulatory elements, between duplicated genes as we observed for *stat1* genes is predicted to occur frequently by neutral evolution due to the reciprocal extinction of regulatory elements in the two duplicates (Force et al., 1999; Postlethwait et al., 2004).

Second, the differential expression patterns of *stat1a* and *stat1b* may reflect different roles in development and physiology. Zebrafish Stat1a can rescue interferon signaling in human tissue culture cells that lack STAT1 activity, showing that Stat1a shares an ancestral virus-related cytokine-signaling mechanism with humans (Oates et al., 1999b). The virus-related function of Stat1 protein is expected to be required broadly in many cell types consistent with the broad expression pattern of *stat1a*. In contrast, *stat1b* expression and gene knockdown analysis reveal a role for *stat1b* in hematopoiesis and this gene is expressed specifically in the hematopoietic lineage.

Knockdown experiments confirmed a role for *stat1b* in zebrafish hematopoiesis. As assayed both by *in situ* hybridization and by quantitative PCR, the knockdown of *stat1b* activity led to the increased expression of *scl* and *gata1* in primitive hematopoiesis and the increase in hemoglobin-producing cells but the decreased expression of *spi* and *mpx*. Because RNA in situ expression analyses showed broadened expression compartments, we conclude that the increased expression of *scl* and *gata1* results from more cells expressing these markers after *stat1b* knockdown than in controls. Likewise, the smaller compartments of *spi* and *mpx* reflect fewer cells expressing these markers after *stat1b* knockdown. The *scl* gene marks primitive hematopoietic stem cells and *gata1* marks erythroid cells, whereas *spi1* and *mpx* mark myeloid cell lineages. The expression compartments of genes marking other lineages, including markers for definitive HSC (*c-myb* and *runx1*), macrophages (*l-plastin*), and lymphoid cells (*rag1*), were unaltered after *stat1b* knockdown. Thus, these results suggest that *stat1b* knockdown results in an increase in cells of the erythroid lineage at the expense of the myeloid lineage.

We interpret these results in the following framework. First, progenitor cells with high *scl* expression may be biased towards erythrocyte differentiation, whereas other markers of primitive HSCs, such as *fli1a, gata2,* and *hhex*, might be responsible for the differentiation of HSCs into other cell lineages, including myeloid and lymphoid cells (de Jong and Zon, 2005). Second, normal Stat1b function may be necessary to promote the myeloid lineage of *spi1*- and *mpx*-expressing cells and/or to suppress the erythroid lineage of *gata1*-expressing, *o*-dianisidine-positive cells. Note that the knockdown of *stat1b* reported here provides a result complementary to that derived from the knockdown of *gata1*, which leads to an increase of *spi1* and *mpx* expression in zebrafish and suggests that *gata1* suppresses the

myeloid pathway (Galloway et al., 2005; Rhodes et al., 2005). Thus, *stat1b* and *gata1* may play opposing roles in hematopoietic cell fate determination.

Whether mammalian STAT1 proteins play a role in hematopoiesis similar to that shown here for *stat1b* in zebrafish is as yet unclear. Recent studies showed that IFN treatments stimulated dormant HSCs in mice and that the effect depended on *Stat1* (Baldridge et al., 2010; Essers et al., 2009; Sato et al., 2009), but the roles of STAT1-alpha and STAT1-beta forms were not tested independently. In addition, IFN--gamma produced by Th1 cells stimulates a significant expansion of LSK (lineage marker minus, Sca-1+, cKit+) hematopoietic stem cells that tend to differentiate into myeloid lineages through a STAT1 dependent pathway in mice (Zhao et al., 2010). In those experiments (Zhao et al., 2010), IFN--gamma led to the depletion of total progenitor cells but to the promotion of LSK cell proliferation into myeloid cells, which then compensated for the loss of total progenitors. IFN--gamma has long been known to regulate hematopoietic cell proliferation (Raefsky et al., 1985) but its effects are complicated. Depending on the stage of hematopoiesis and the hematopoietic lineage, IFN-gamma either inhibits hematopoiesis (Shimozato et al., 2002; Young et al., 1997) or promotes the expansion of specific stem cell populations and the differentiation of myeloid cells (Brugger et al., 1993; Caux et al., 1992), in each case mediated by STAT1. These results suggest the hypothesis that the basic functions we found for *stat1b* in myeloid development may be shared by the mammalian orthologs.

In our experiments, Stat1b could act in any of a number of ways. It might (1) promote the apoptosis of erythroid cells, which is unlikely given our apoptosis studies; (2) inhibit the differentiation of progenitor cells into erythrocytes; or (3) promote the differentiation of progenitor cells into myeloid cells. Further investigation of the regulatory effects of IFN and STAT1 in various hematopoietic cell lineages and at different developmental stages would shed light on the mechanisms by which those two important regulators act in normal development and perhaps in the bone marrow failure and myeloid cancers of Fanconi anemia patients. The partitioning of ancestral STAT1 functions between the zebrafish *stat1a* and *stat1b* gene duplicates provide a special opportunity to dissect the complicated hematopoietic roles of STAT1 genes in developing vertebrate embryos.

4. Experimental Procedures

4.1. Primers for cloning stat1b cDNA

Primers covering overlapping fragments of XR_029517 were designed for RT-PCR, with two primer pairs for each fragment. PCR products were cloned with the TOPO TA cloning kit into the pCR4-TOPO vector (Invitrogen, Carlsbad, CA, USA) and sequences were assembled to obtain a full-length cDNA sequence. Primers: stat1bF10 CGTTGAAAGATGACGCTCTG, stat1bR10 ACGGATCTGCTGGAGACACT; stat1bF11 GCTTATCCCGAGATACACTCC, stat1bR11 TCTTCAGCTGCTGACGGATCT; stat1bF20 GCTGAAGGTGTGCAAATGAA, stat1bR20 AGGCACTGGGTAACTGGTTG; stat1bF21 GCTGAAGGTGTGCAAATGAA, stat1bR21 TTCACCGCTGAGCATGTTGTA; stat1bF30 GACGCCTCTCATCGTTACAGA, stat1bR30 TTTTGGGATGTTCGGGTAAA; stat1bF31 GCAGCTGAATTTCGTCATTTG, stat1bR31 GCGACCAAAAGCTTCATCTT; stat1bF40 TGGTGAACCCAAGATCCATT, stat1bR40 GTGAAATGGCCTGTTCATCC; stat1bF41 TGCGCTTTAGTGAAAGCTGT, stat1bR41 TGAAATGGCCTGTTCATCCA; stat1bF50 CAGCAGATGGCTTGTATTGG, stat1bR50 TGCCAGCTTATGACCTTTGA; stat1bF51 TATCAGAGGAGTTACCCGAGT, stat1bR51 TGCTGATTGAAGAAAACTGCC.

4.2. Phylogenetic analysis

For phylogenetic analysis, STAT-related protein sequences were downloaded from NCBI and from Ensembl and were aligned by Muscle (MUltiple Sequence Comparison by Log-Expectation, http://www.ebi.ac.uk/Tools/muscle/index.html) using the JTT model (Abascal et al., 2005). PhyML (Guindon and Gascuel, 2003); http://www.atgc-montpellier.fr/phyml/) was used to construct maximum likelihood phylogenetic trees.

4.3. Zebrafish, morpholinos, and in situ hybridization

Zebrafish (ABC X TU strain) were maintained as described (Kimmel et al., 1995) with all protocols approved by the University of Oregon IACUC. The *stat1b* morpholino (AAAATGTAGCGGATGTTACTTCGAC, Gene Tools, LLC, Philomath, OR, USA) targets the splice donor site of exon-5-intron-5, leading to the inclusion of intron-5 and a premature translation stop codon. The *stat1a* MO (TCATGTGGTCAACAGGCACCTGCAA) targets the splice donor site of exon-3-intron-3, leading to the inclusion of intron-3 and a premature translation stop. The sequence of the control MO was CCTCTTACCTCAGTTACAATTTATA, which has no significant similarity in the zebrafish reference genome sequence database. A volume of 2nl of MO (5 mg/ml for *stat1b* MO and 10 mg/ml for *stat1a* MO and control MO) was injected into one-cell stage embryos.

For RNA *in situ* hybridization, embryos were collected at various ages and queried using as probe the 3′ untranslated regions of zebrafish *stat1a* and *stat1b*, and as negative control a cuttlefish sequence (GenBank: **GU388435**). RNA *in situ* hybridization with all three probes was carried out following methods previously described (Yan et al., 2002) except that *stat1b* probe was incubated at 50°C. RNA *in situ* hybridization with blood markers was carried out at 16 hpf and 32 hpf following methods previously described (Yan et al., 2002).

4.4. RT-PCR and Quantitative RT-PCR

Fertilized eggs were collected at indicated time points. Total RNA was extracted with TRI reagent (Molecular Research Center, Cincinnati, OH, USA) and genomic DNA was removed with DNA-free™ DNase Treatment and Removal Reagents (ABI, Foster City, CA, USA). Total RNA was quantified by spectrometry at 260 nm to ensure equal loading for RT-PCR. Product from each pair of primers was sequenced and verified to be the target mRNA fragment before the actual RT-PCR. RT-PCR was run with the OneStep RT-PCR kit (QIAGEN, Valencia, CA, USA). Primers used were: actinF GCCAACACAGTGCTGTCTGGAGG, actinR GGTCATGGACGCCCATTGTGAGG; stat1aMEF AGTCGCAGCAATGACTCAGTG, stat1aMER CTGCTGATGATCATCGCCATTG; stat1bMEF AGGTGACTCCATGCAGGGGAAC, stat1bMER GCGGGTCGTTGCTGTAGGTGA. cDNAs were prepared with the High Capacity RNA-to-cDNA kit (ABI, Foster City, CA, USA). Quantitative PCR was carried out using Power SYBR® Green PCR Master Mix (ABI, Foster City, CA, USA). Q-PCR was run with three biological repeats and three sampling repeats. The expression level of a house-keeping gene zgc:136952 (GenBank: **NM_001040043**), which encodes RPL32 (ribosomal protein L32) was run as an internal control. After collection, raw Ct data were normalized to that of this internal control. The expression level of each marker gene in control MO, *stat1a* MO, and *stat1b* MO treated embryos was then compared with a *t*-test assuming equal standard deviations with $\alpha = 0.05$ (95% confidence interval). Primers used were: gata1qF GAATGCAGCTTCAGAGGTTTATCC, gata1qR TGGGTTCAGAGAATACGCTCCTA; mpxqF CCAAACCTCAGGGATGTTCTTG, mpxqR CCCAAACTACGAGTCCCTATGC; spiqF GGGTAGCCATCACATCCCTCTAG, spiqR TGGACGTTGTGAGGGTAACACA; sclqF GACTAATTTCTCGGGCTGACAACTA, sclqR

GGGCGTTAACAGAAAGTCTTACGTA; RPL32qF CCCTCACCAAACCTAAGATCGT, RPL32qR CTCCAGTTTGCCCTGATCTTG.

4.5 Acridine orange and o-dianisidine staining

For analyses of cell death, 30 hpf embryos were dechorionated by hand and treated with 0.5 ug/ml acridine orange in embryo media for 30 minutes, washed 3x with embryo media, anesthetized with MS-222. For analyses of hemoglobin production, dechorionated embryos at 30 hpf and 48hpf were anesthetized, and treated with 0.06% o-dianisidine in 40% ethanol, 0.01M NaOAc, pH 4.5 and 0.6% of H_2O_2 for 15 minutes at room temperature in the dark. Embryos were washed with PBT to stop the reaction and fixed in 4% paraformaldehyde. After acridine orange and *o*-dianisidine treatments, embryos were imaged on a Leica spinning disc confocal microscope. Images were opened in ImageJ, max-projected, and red pixels in the ICM were counted.

Supplementary Material

Refer to Web version on PubMed Central for supplementary material.

References

Abascal F, Zardoya R, Posada D. ProtTest: selection of best-fit models of protein evolution. Bioinformatics. 2005; 21:2104–5. [PubMed: 15647292]

Altschul SF, Koonin EV. Iterated profile searches with PSI-BLAST--a tool for discovery in protein databases. Trends Biochem Sci. 1998; 23:444–7. [PubMed: 9852764]

Amores A, Force A, Yan YL, Joly L, Amemiya C, Fritz A, Ho RK, Langeland J, Prince V, Wang YL, Westerfield M, Ekker M, Postlethwait JH. Zebrafish hox clusters and vertebrate genome evolution. Science. 1998; 282:1711–4. [PubMed: 9831563]

Amores A, Suzuki T, Yan YL, Pomeroy J, Singer A, Amemiya C, Postlethwait JH. Developmental roles of pufferfish Hox clusters and genome evolution in ray-fin fish. Genome Res. 2004; 14:1–10. [PubMed: 14707165]

Aronica MG, Brizzi MF, Dentelli P, Rosso A, Yarden Y, Pegoraro L. p91 STAT1 activation in interleukin-3-stimulated primary acute myeloid leukemia cells. Oncogene. 1996; 13:1017–26. [PubMed: 8806691]

Baldridge MT, King KY, Boles NC, Weksberg DC, Goodell MA. Quiescent haematopoietic stem cells are activated by IFN-gamma in response to chronic infection. Nature. 2010; 465:793–7. [PubMed: 20535209]

Baran-Marszak F, Feuillard J, Najjar I, Le Clorennec C, Bechet JM, Dusanter-Fourt I, Bornkamm GW, Raphael M, Fagard R. Differential roles of STAT1alpha and STAT1beta in fludarabine-induced cell cycle arrest and apoptosis in human B cells. Blood. 2004; 104:2475–83. [PubMed: 15217838]

Becker S, Groner B, Muller CW. Three-dimensional structure of the Stat3beta homodimer bound to DNA. Nature. 1998; 394:145–51. [PubMed: 9671298]

Bennett CM, Kanki JP, Rhodes J, Liu TX, Paw BH, Kieran MW, Langenau DM, Delahaye-Brown A, Zon LI, Fleming MD, Look AT. Myelopoiesis in the zebrafish, Danio rerio. Blood. 2001; 98:643–51. [PubMed: 11468162]

Bertrand JY, Traver D. Hematopoietic cell development in the zebrafish embryo. Curr Opin Hematol. 2009; 16:243–8. [PubMed: 19491671]

Brierley MM, Fish EN. Stats: multifaceted regulators of transcription. J Interferon Cytokine Res. 2005; 25:733–44. [PubMed: 16375601]

Bromberg JF, Fan Z, Brown C, Mendelsohn J, Darnell JE Jr. Epidermal growth factor-induced growth inhibition requires Stat1 activation. Cell Growth Differ. 1998; 9:505–12. [PubMed: 9690618]

Bromberg JF, Horvath CM, Wen Z, Schreiber RD, Darnell JE Jr. Transcriptionally active Stat1 is required for the antiproliferative effects of both interferon alpha and interferon gamma. Proc Natl Acad Sci U S A. 1996; 93:7673–8. [PubMed: 8755534]

Brugger W, Mocklin W, Heimfeld S, Berenson RJ, Mertelsmann R, Kanz L. Ex vivo expansion of enriched peripheral blood CD34+ progenitor cells by stem cell factor, interleukin-1 beta (IL-1 beta), IL-6, IL-3, interferon-gamma, and erythropoietin. Blood. 1993; 81:2579–84. [PubMed: 7683923]

Burns CE, Traver D, Mayhall E, Shepard JL, Zon LI. Hematopoietic stem cell fate is established by the Notch-Runx pathway. Genes Dev. 2005; 19:2331–42. [PubMed: 16166372]

Catchen JM, Conery JS, Postlethwait JH. Automated identification of conserved synteny after whole-genome duplication. Genome Res. 2009; 19:1497–505. [PubMed: 19465509]

Caux C, Moreau I, Saeland S, Banchereau J. Interferon-gamma enhances factor-dependent myeloid proliferation of human CD34+ hematopoietic progenitor cells. Blood. 1992; 79:2628–35. [PubMed: 1375107]

Chen X, Vinkemeier U, Zhao Y, Jeruzalmi D, Darnell JE Jr, Kuriyan J. Crystal structure of a tyrosine phosphorylated STAT-1 dimer bound to DNA. Cell. 1998; 93:827–39. [PubMed: 9630226]

Chin YE, Kitagawa M, Su WC, You ZH, Iwamoto Y, Fu XY. Cell growth arrest and induction of cyclin-dependent kinase inhibitor p21 WAF1/CIP1 mediated by STAT1. Science. 1996; 272:719–22. [PubMed: 8614832]

Ciau-Uitz A, Liu F, Patient R. Genetic control of hematopoietic development in Xenopus and zebrafish. Int J Dev Biol. 2010; 54:1139–49. [PubMed: 20711991]

Crispino JD. GATA1 in normal and malignant hematopoiesis. Semin Cell Dev Biol. 2005; 16:137–47. [PubMed: 15659348]

Davidson AJ, Ernst P, Wang Y, Dekens MP, Kingsley PD, Palis J, Korsmeyer SJ, Daley GQ, Zon LI. cdx4 mutants fail to specify blood progenitors and can be rescued by multiple hox genes. Nature. 2003; 425:300–6. [PubMed: 13679919]

de Jong JL, Zon LI. Use of the zebrafish system to study primitive and definitive hematopoiesis. Annu Rev Genet. 2005; 39:481–501. [PubMed: 16285869]

Decker T, Kovarik P. Serine phosphorylation of STATs. Oncogene. 2000; 19:2628–37. [PubMed: 10851062]

Dehal P, Boore JL. Two rounds of whole genome duplication in the ancestral vertebrate. PLoS Biol. 2005; 3:e314. [PubMed: 16128622]

Detrich HW 3rd, Kieran MW, Chan FY, Barone LM, Yee K, Rundstadler JA, Pratt S, Ransom D, Zon LI. Intraembryonic hematopoietic cell migration during vertebrate development. Proc Natl Acad Sci U S A. 1995; 92:10713–7. [PubMed: 7479870]

Durbin JE, Hackenmiller R, Simon MC, Levy DE. Targeted disruption of the mouse Stat1 gene results in compromised innate immunity to viral disease. Cell. 1996; 84:443–50. [PubMed: 8608598]

Ellett F, Lieschke GJ. Zebrafish as a model for vertebrate hematopoiesis. Curr Opin Pharmacol. 2010; 10:563–70. [PubMed: 20538521]

Essers MA, Offner S, Blanco-Bose WE, Waibler Z, Kalinke U, Duchosal MA, Trumpp A. IFNalpha activates dormant haematopoietic stem cells in vivo. Nature. 2009; 458:904–8. [PubMed: 19212321]

Force A, Lynch M, Pickett FB, Amores A, Yan YL, Postlethwait J. Preservation of duplicate genes by complementary, degenerative mutations. Genetics. 1999; 151:1531–45. [PubMed: 10101175]

Forrai A, Robb L. The hemangioblast--between blood and vessels. Cell Cycle. 2003; 2:86–90. [PubMed: 12695653]

Fujiwara Y, Browne CP, Cunniff K, Goff SC, Orkin SH. Arrested development of embryonic red cell precursors in mouse embryos lacking transcription factor GATA-1. Proc Natl Acad Sci U S A. 1996; 93:12355–8. [PubMed: 8901585]

Galloway JL, Wingert RA, Thisse C, Thisse B, Zon LI. Loss of gata1 but not gata2 converts erythropoiesis to myelopoiesis in zebrafish embryos. Dev Cell. 2005; 8:109–16. [PubMed: 15621534]

Georgopoulos K, Winandy S, Avitahl N. The role of the Ikaros gene in lymphocyte development and homeostasis. Annu Rev Immunol. 1997; 15:155–76. [PubMed: 9143685]

Gouilleux-Gruart V, Debierre-Grockiego F, Gouilleux F, Capiod JC, Claisse JF, Delobel J, Prin L. Activated Stat related transcription factors in acute leukemia. Leuk Lymphoma. 1997; 28:83–8. [PubMed: 9498707]

Guindon S, Gascuel O. A simple, fast, and accurate algorithm to estimate large phylogenies by maximum likelihood. Syst Biol. 2003; 52:696–704. [PubMed: 14530136]

Haneline LS, Broxmeyer HE, Cooper S, Hangoc G, Carreau M, Buchwald M, Clapp DW. Multiple inhibitory cytokines induce deregulated progenitor growth and apoptosis in hematopoietic cells from Fac−/− mice. Blood. 1998; 91:4092–8. [PubMed: 9596654]

Herbomel P, Thisse B, Thisse C. Ontogeny and behaviour of early macrophages in the zebrafish embryo. Development. 1999; 126:3735–45. [PubMed: 10433904]

Holland PWH, Garcia-Fernàndez J, Williams NA, Sidow A. Gene duplications and the origins of vertebrate development. Development. 1994:125–133.

Improta T, Schindler C, Horvath CM, Kerr IM, Stark GR, Darnell JE Jr. Transcription factor ISGF-3 formation requires phosphorylated Stat91 protein, but Stat113 protein is phosphorylated independently of Stat91 protein. Proc Natl Acad Sci U S A. 1994; 91:4776–80. [PubMed: 8197134]

Isogai S, Horiguchi M, Weinstein BM. The vascular anatomy of the developing zebrafish: an atlas of embryonic and early larval development. Dev Biol. 2001; 230:278–301. [PubMed: 11161578]

Jaillon O, Aury JM, Brunet F, Petit JL, Stange-Thomann N, Mauceli E, Bouneau L, Fischer C, Ozouf-Costaz C, Bernot A, Nicaud S, Jaffe D, Fisher S, Lutfalla G, Dossat C, Segurens B, Dasilva C, Salanoubat M, Levy M, Boudet N, Castellano S, Anthouard V, Jubin C, Castelli V, Katinka M, Vacherie B, Biemont C, Skalli Z, Cattolico L, Poulain J, De Berardinis V, Cruaud C, Duprat S, Brottier P, Coutanceau JP, Gouzy J, Parra G, Lardier G, Chapple C, McKernan KJ, McEwan P, Bosak S, Kellis M, Volff JN, Guigo R, Zody MC, Mesirov J, Lindblad-Toh K, Birren B, Nusbaum C, Kahn D, Robinson-Rechavi M, Laudet V, Schachter V, Quetier F, Saurin W, Scarpelli C, Wincker P, Lander ES, Weissenbach J, Roest Crollius H. Genome duplication in the teleost fish Tetraodon nigroviridis reveals the early vertebrate proto-karyotype. Nature. 2004; 431:946–57. [PubMed: 15496914]

Kalev-Zylinska ML, Horsfield JA, Flores MV, Postlethwait JH, Vitas MR, Baas AM, Crosier PS, Crosier KE. Runx1 is required for zebrafish blood and vessel development and expression of a human RUNX1-CBF2T1 transgene advances a model for studies of leukemogenesis. Development. 2002; 129:2015–30. [PubMed: 11934867]

Kane DA, Kimmel CB. The zebrafish midblastula transition. Development. 1993; 119:447–56. [PubMed: 8287796]

Kastner P, Chan S. PU.1: a crucial and versatile player in hematopoiesis and leukemia. Int J Biochem Cell Biol. 2008; 40:22–7. [PubMed: 17374502]

Kimmel CB, Ballard WW, Kimmel SR, Ullmann B, Schilling TF. Stages of embryonic development of the zebrafish. Dev Dyn. 1995; 203:253–310. [PubMed: 8589427]

Kisseleva T, Bhattacharya S, Braunstein J, Schindler CW. Signaling through the JAK/STAT pathway, recent advances and future challenges. Gene. 2002; 285:1–24. [PubMed: 12039028]

Lewis RS, Ward AC. Conservation, duplication and divergence of the zebrafish stat5 genes. Gene. 2004; 338:65–74. [PubMed: 15302407]

Li X, Yang Y, Yuan J, Hong P, Freie B, Orazi A, Haneline LS, Clapp DW. Continuous in vivo infusion of interferon-gamma (IFN-gamma) preferentially reduces myeloid progenitor numbers and enhances engraftment of syngeneic wild-type cells in Fancc−/− mice. Blood. 2004; 104:1204–9. [PubMed: 15113761]

Liao EC, Paw BH, Oates AC, Pratt SJ, Postlethwait JH, Zon LI. SCL/Tal-1 transcription factor acts downstream of cloche to specify hematopoietic and vascular progenitors in zebrafish. Genes Dev. 1998; 12:621–6. [PubMed: 9499398]

Lieschke GJ, Oates AC, Paw BH, Thompson MA, Hall NE, Ward AC, Ho RK, Zon LI, Layton JE. Zebrafish SPI-1 (PU.1) marks a site of myeloid development independent of primitive erythropoiesis: implications for axial patterning. Dev Biol. 2002; 246:274–95. [PubMed: 12051816]

Long Q, Meng A, Wang H, Jessen JR, Farrell MJ, Lin S. GATA-1 expression pattern can be recapitulated in living transgenic zebrafish using GFP reporter gene. Development. 1997; 124:4105–11. [PubMed: 9374406]

Marchler-Bauer A, Anderson JB, Chitsaz F, Derbyshire MK, DeWeese-Scott C, Fong JH, Geer LY, Geer RC, Gonzales NR, Gwadz M, He S, Hurwitz DI, Jackson JD, Ke Z, Lanczycki CJ, Liebert CA, Liu C, Lu F, Lu S, Marchler GH, Mullokandov M, Song JS, Tasneem A, Thanki N, Yamashita RA, Zhang D, Zhang N, Bryant SH. CDD: specific functional annotation with the Conserved Domain Database. Nucleic Acids Res. 2009; 37:D205–10. [PubMed: 18984618]

Meraz MA, White JM, Sheehan KC, Bach EA, Rodig SJ, Dighe AS, Kaplan DH, Riley JK, Greenlund AC, Campbell D, Carver-Moore K, DuBois RN, Clark R, Aguet M, Schreiber RD. Targeted disruption of the Stat1 gene in mice reveals unexpected physiologic specificity in the JAK-STAT signaling pathway. Cell. 1996; 84:431–42. [PubMed: 8608597]

Mowen KA, Tang J, Zhu W, Schurter BT, Shuai K, Herschman HR, David M. Arginine methylation of STAT1 modulates IFNalpha/beta-induced transcription. Cell. 2001; 104:731–41. [PubMed: 11257227]

Muller M, Laxton C, Briscoe J, Schindler C, Improta T, Darnell JE Jr, Stark GR, Kerr IM. Complementation of a mutant cell line: central role of the 91 kDa polypeptide of ISGF3 in the interferon-alpha and -gamma signal transduction pathways. EMBO J. 1993; 12:4221–8. [PubMed: 7693454]

Najjar I, Deglesne PA, Schischmanoff PO, Fabre EE, Boisson-Dupuis S, Nimmerjahn F, Bornkamm GW, Dusanter-Fourt I, Fagard R. STAT1-dependent IgG cell-surface expression in a human B cell line derived from a STAT1-deficient patient. J Leukoc Biol. 2010; 87:1145–52. [PubMed: 20200400]

Najjar I, Fagard R. STAT1 and pathogens, not a friendly relationship. Biochimie. 2010; 92:425–44. [PubMed: 20159032]

Najjar I, Schischmanoff PO, Baran-Marszak F, Deglesne PA, Youlyouz-Marfak I, Pampin M, Feuillard J, Bornkamm GW, Chelbi-Alix MK, Fagard R. Novel function of STAT1beta in B cells: induction of cell death by a mechanism different from that of STAT1alpha. J Leukoc Biol. 2008; 84:1604–12. [PubMed: 18753311]

Oates AC, Brownlie A, Pratt SJ, Irvine DV, Liao EC, Paw BH, Dorian KJ, Johnson SL, Postlethwait JH, Zon LI, Wilks AF. Gene duplication of zebrafish JAK2 homologs is accompanied by divergent embryonic expression patterns: only jak2a is expressed during erythropoiesis. Blood. 1999a; 94:2622–36. [PubMed: 10515866]

Oates AC, Wollberg P, Pratt SJ, Paw BH, Johnson SL, Ho RK, Postlethwait JH, Zon LI, Wilks AF. Zebrafish stat3 is expressed in restricted tissues during embryogenesis and stat1 rescues cytokine signaling in a STAT1-deficient human cell line. Dev Dyn. 1999b; 215:352–70. [PubMed: 10417824]

Ohno, S. Evolution by Gene Duplication. Springer-Verlag; New York: 1970.

Oikawa T, Yamada T, Kihara-Negishi F, Yamamoto H, Kondoh N, Hitomi Y, Hashimoto Y. The role of Ets family transcription factor PU.1 in hematopoietic cell differentiation, proliferation and apoptosis. Cell Death Differ. 1999; 6:599–608. [PubMed: 10453070]

Otsuki T, Nagakura S, Wang J, Bloom M, Grompe M, Liu JM. Tumor necrosis factor-alpha and CD95 ligation suppress erythropoiesis in Fanconi anemia C gene knockout mice. J Cell Physiol. 1999; 179:79–86. [PubMed: 10082135]

Paik EJ, Zon LI. Hematopoietic development in the zebrafish. Int J Dev Biol. 2010; 54:1127–37. [PubMed: 20711990]

Pang Q, Fagerlie S, Christianson TA, Keeble W, Faulkner G, Diaz J, Rathbun RK, Bagby GC. The Fanconi anemia protein FANCC binds to and facilitates the activation of STAT1 by gamma interferon and hematopoietic growth factors. Mol Cell Biol. 2000; 20:4724–35. [PubMed: 10848598]

Patterson LJ, Gering M, Patient R. Scl is required for dorsal aorta as well as blood formation in zebrafish embryos. Blood. 2005; 105:3502–11. [PubMed: 15644413]

Postlethwait J, Amores A, Cresko W, Singer A, Yan YL. Subfunction partitioning, the teleost radiation and the annotation of the human genome. Trends Genet. 2004; 20:481–90. [PubMed: 15363902]

Postlethwait JH, Yan YL, Gates MA, Horne S, Amores A, Brownlie A, Donovan A, Egan ES, Force A, Gong Z, Goutel C, Fritz A, Kelsh R, Knapik E, Liao E, Paw B, Ransom D, Singer A, Thomson M, Abduljabbar TS, Yelick P, Beier D, Joly JS, Larhammar D, Rosa F, Westerfield M, Zon LI,

Johnson SL, Talbot WS. Vertebrate genome evolution and the zebrafish gene map. Nat Genet. 1998; 18:345–9. [PubMed: 9537416]

Raefsky EL, Platanias LC, Zoumbos NC, Young NS. Studies of interferon as a regulator of hematopoietic cell proliferation. J Immunol. 1985; 135:2507–12. [PubMed: 2411798]

Rathbun RK, Faulkner GR, Ostroski MH, Christianson TA, Hughes G, Jones G, Cahn R, Maziarz R, Royle G, Keeble W, Heinrich MC, Grompe M, Tower PA, Bagby GC. Inactivation of the Fanconi anemia group C gene augments interferon-gamma-induced apoptotic responses in hematopoietic cells. Blood. 1997; 90:974–85. [PubMed: 9242526]

Rhodes J, Hagen A, Hsu K, Deng M, Liu TX, Look AT, Kanki JP. Interplay of pu.1 and gata1 determines myelo-erythroid progenitor cell fate in zebrafish. Dev Cell. 2005; 8:97–108. [PubMed: 15621533]

Sato T, Onai N, Yoshihara H, Arai F, Suda T, Ohteki T. Interferon regulatory factor-2 protects quiescent hematopoietic stem cells from type I interferon-dependent exhaustion. Nat Med. 2009; 15:696–700. [PubMed: 19483695]

Schindler C, Fu XY, Improta T, Aebersold R, Darnell JE Jr. Proteins of transcription factor ISGF-3: one gene encodes the 91-and 84-kDa ISGF-3 proteins that are activated by interferon alpha. Proc Natl Acad Sci U S A. 1992; 89:7836–9. [PubMed: 1502203]

Schmitt C, Tonnelle C, Dalloul A, Chabannon C, Debre P, Rebollo A. Aiolos and Ikaros: regulators of lymphocyte development, homeostasis and lymphoproliferation. Apoptosis. 2002; 7:277–84. [PubMed: 11997672]

Shimozato O, Ortaldo JR, Komschlies KL, Young HA. Impaired NK cell development in an IFN-gamma transgenic mouse: aberrantly expressed IFN-gamma enhances hematopoietic stem cell apoptosis and affects NK cell differentiation. J Immunol. 2002; 168:1746–52. [PubMed: 11823506]

Shivdasani RA, Mayer EL, Orkin SH. Absence of blood formation in mice lacking the T-cell leukaemia oncoprotein tal-1/SCL. Nature. 1995; 373:432–4. [PubMed: 7830794]

Si Y, Ciccone S, Yang FC, Yuan J, Zeng D, Chen S, van de Vrugt HJ, Critser J, Arwert F, Haneline LS, Clapp DW. Continuous in vivo infusion of interferon-gamma (IFN-gamma) enhances engraftment of syngeneic wild-type cells in Fanca−/− and Fancg−/− mice. Blood. 2006; 108:4283–7. [PubMed: 16946306]

Song HD, Sun XJ, Deng M, Zhang GW, Zhou Y, Wu XY, Sheng Y, Chen Y, Ruan Z, Jiang CL, Fan HY, Zon LI, Kanki JP, Liu TX, Look AT, Chen Z. Hematopoietic gene expression profile in zebrafish kidney marrow. Proc Natl Acad Sci U S A. 2004; 101:16240–5. [PubMed: 15520368]

Stark GR, Kerr IM, Williams BR, Silverman RH, Schreiber RD. How cells respond to interferons. Annu Rev Biochem. 1998; 67:227–64. [PubMed: 9759489]

Sullivan C, Charette J, Catchen J, Lage CR, Giasson G, Postlethwait JH, Millard PJ, Kim CH. The gene history of zebrafish tlr4a and tlr4b is predictive of their divergent functions. J Immunol. 2009; 183:5896–908. [PubMed: 19812203]

Taylor JS, Braasch I, Frickey T, Meyer A, Van de Peer Y. Genome duplication, a trait shared by 22000 species of ray-finned fish. Genome Res. 2003; 13:382–90. [PubMed: 12618368]

Thompson MA, Ransom DG, Pratt SJ, MacLennan H, Kieran MW, Detrich HW 3rd, Vail B, Huber TL, Paw B, Brownlie AJ, Oates AC, Fritz A, Gates MA, Amores A, Bahary N, Talbot WS, Her H, Beier DR, Postlethwait JH, Zon LI. The cloche and spadetail genes differentially affect hematopoiesis and vasculogenesis. Dev Biol. 1998; 197:248–69. [PubMed: 9630750]

Traver D. Cellular dissection of zebrafish hematopoiesis. Methods Cell Biol. 2004; 76:127–49. [PubMed: 15602875]

Vignais ML, Sadowski HB, Watling D, Rogers NC, Gilman M. Platelet-derived growth factor induces phosphorylation of multiple JAK family kinases and STAT proteins. Mol Cell Biol. 1996; 16:1759–69. [PubMed: 8657151]

Vinkemeier U, Moarefi I, Darnell JE Jr, Kuriyan J. Structure of the amino-terminal protein interaction domain of STAT-4. Science. 1998; 279:1048–52. [PubMed: 9461439]

Weber-Nordt RM, Egen C, Wehinger J, Ludwig W, Gouilleux-Gruart V, Mertelsmann R, Finke J. Constitutive activation of STAT proteins in primary lymphoid and myeloid leukemia cells and in

Epstein-Barr virus (EBV)-related lymphoma cell lines. Blood. 1996; 88:809–16. [PubMed: 8704235]

Whitney MA, Royle G, Low MJ, Kelly MA, Axthelm MK, Reifsteck C, Olson S, Braun RE, Heinrich MC, Rathbun RK, Bagby GC, Grompe M. Germ cell defects and hematopoietic hypersensitivity to gamma-interferon in mice with a targeted disruption of the Fanconi anemia C gene. Blood. 1996; 88:49–58. [PubMed: 8704201]

Willett CE, Cherry JJ, Steiner LA. Characterization and expression of the recombination activating genes (rag1 and rag2) of zebrafish. Immunogenetics. 1997; 45:394–404. [PubMed: 9089097]

Xiong JW. Molecular and developmental biology of the hemangioblast. Dev Dyn. 2008; 237:1218–31. [PubMed: 18429046]

Yan YL, Miller CT, Nissen RM, Singer A, Liu D, Kirn A, Draper B, Willoughby J, Morcos PA, Amsterdam A, Chung BC, Westerfield M, Haffter P, Hopkins N, Kimmel C, Postlethwait JH. A zebrafish sox9 gene required for cartilage morphogenesis. Development. 2002; 129:5065–79. [PubMed: 12397114]

Yang E, Henriksen MA, Schaefer O, Zakharova N, Darnell JE Jr. Dissociation time from DNA determines transcriptional function in a STAT1 linker mutant. J Biol Chem. 2002; 277:13455–62. [PubMed: 11834743]

Young HA, Klinman DM, Reynolds DA, Grzegorzewski KJ, Nii A, Ward JM, Winkler-Pickett RT, Ortaldo JR, Kenny JJ, Komschlies KL. Bone marrow and thymus expression of interferon-gamma results in severe B-cell lineage reduction, T-cell lineage alterations, and hematopoietic progenitor deficiencies. Blood. 1997; 89:583–95. [PubMed: 9002962]

Zakharova N, Lymar ES, Yang E, Malik S, Zhang JJ, Roeder RG, Darnell JE Jr. Distinct transcriptional activation functions of STAT1alpha and STAT1beta on DNA and chromatin templates. J Biol Chem. 2003; 278:43067–73. [PubMed: 12939262]

Zhang X, Li J, Sejas DP, Rathbun KR, Bagby GC, Pang Q. The Fanconi anemia proteins functionally interact with the protein kinase regulated by RNA (PKR). J Biol Chem. 2004; 279:43910–9. [PubMed: 15299030]

Zhao X, Ren G, Liang L, Ai PZ, Zheng B, Tischfield JA, Shi Y, Shao C. Brief report: interferon-gamma induces expansion of Lin(−)Sca-1(+)C-Kit(+) Cells. Stem Cells. 2010; 28:122–6. [PubMed: 19890981]

Highlights Stat1b

- Zebrafish has co-orthologs of human *STAT1: stat1a* like STAT1α and *stat1b* like STAT1β.
- STAT1α and STAT1β are splice isoforms but *stat1a* and *stat1b* are 2 duplicated genes.
- *stat1b* but not *stat1a* expression was detected in embryonic hematopoietic tissues.
- *stat1b* but not *stat1a* knockdown decreased myeloid and increased erythrocyte markers.
- Conclusion: zebrafish Stat1b promotes myeloid at expense of erythroid development.

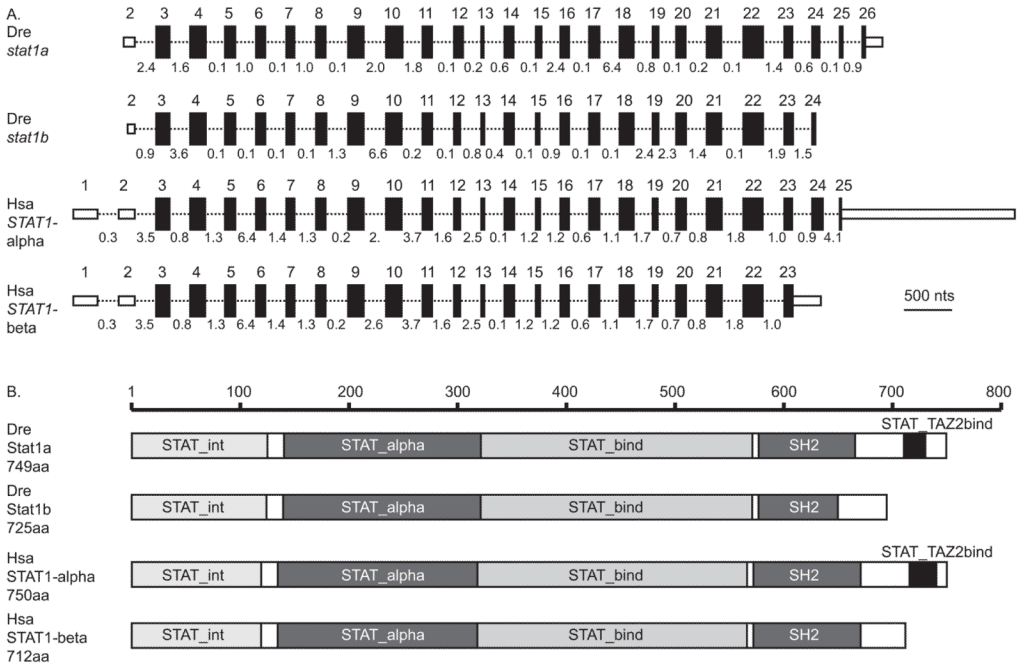

Figure 1.

A comparison of zebrafish and human *STAT1*-related genes and proteins. A. The structure of *STAT1*-related genes. Exons are represented as boxes; small, unfilled boxes represent 3′ and 5′ UTRs and filled boxes represent translated regions. The length of each box is proportional to the length of each exon. Introns are represented as thin dotted lines connecting boxes; the length of each intron is indicated in kilobases but introns are not drawn to scale. B. The structure of STAT1-related proteins. Domains that characterize STAT proteins are marked on diagrams representing lengths in amino acid residues according to the scale bar for proteins encoded by the two zebrafish genes *stat1a* and *stat1b* and the two human STAT1 splicing isoforms STAT1-alpha and STAT1-beta. White boxes represent linker regions between domains. The human STAT1-alpha splice form and the zebrafish Stat1a protein possess a trans-activation domain lacking from the human STAT1-beta splice form and the zebrafish Stat1b protein. This trans-activation domain is approximately 20 amino acids long and it binds selectively to the TAZ2 domain of CREB-binding protein to act as a transcriptional activator. Abbreviations: Dre, *Danio rerio*; Hsa, *Homo sapiens*; SH2, Src homology-2 domain; STAT_alpha, alpha helical, coiled-coil domain; STAT_bind, DNA binding domain; STAT_int, STAT dimer interaction stabilization domain; STAT_TAZ2bind, trans-activation domain.

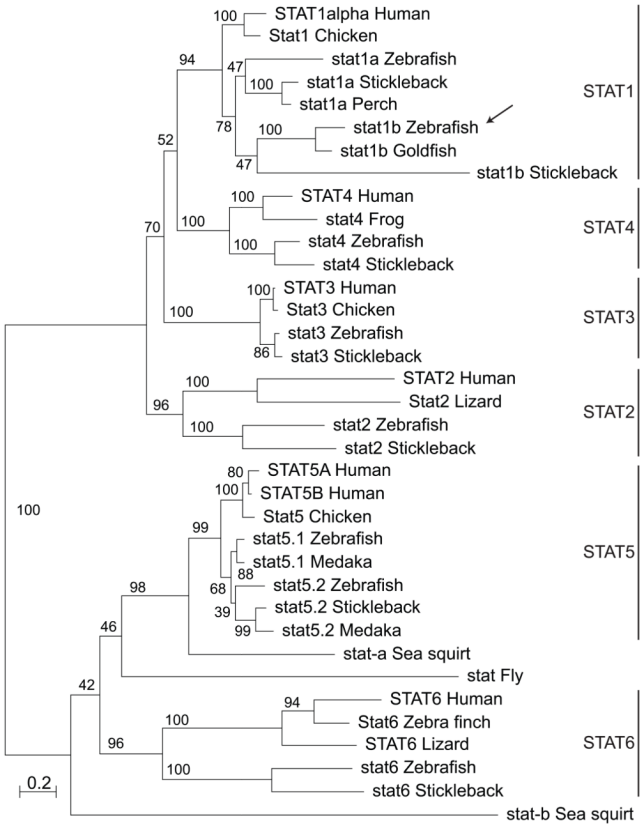

Figure 2.

Phylogenetic analysis of vertebrate STAT proteins: a maximum likelihood tree. The arrow indicates the zebrafish Stat1b protein, which groups as expected if the Stat1b and Stat1a clades arose in the teleost genome duplication event. Bootstrap values as a percent of 100 repetitions. Abbreviations and gene designators (those beginning with ENS are from Ensembl): Chicken (*Gallus gallus*) Stat1 (ENSGALG00000007651), Stat3 (ENSGALG00000003267), Stat5 (ENSGALT00000039892); Fly (*Drosophila melanogaster*) Stat92E-RG; Frog (*Xenopus tropicalis*): stat4 (ENSXETT00000010127); Goldfish (*Carassius auratus*) stat1b (GenBank: **AAO88245**); Human (*Homo sapiens*) STAT1alpha (ENST00000361099), STAT2 (ENST00000314128), STAT3 (ENST00000264657), STAT4 (ENST00000358470), STAT5A (ENST00000345506), STAT5B (ENST00000293328), STAT6 (ENST00000300134); Lizard (*Anolis carolinensis*): STAT2 (ENSACAG00000016385); STAT6 (ENSACAG00000009680); Medaka (*Oryzias latipes*) stat5.1 (ENSORLT00000004951), stat5.2 (ENSORLT00000017980); Perch (*Siniperca chuatsi*) stat1a (GenBank: **ACU12484**) Sea squirt (*Ciona intestinalis*) stat-a (ENSCINT00000020503), stat5 (ENSCING00000004044); Stickleback (*Gasterosteus aculeatus*) stat1a (ENSGACT00000020606), stat1b (ENSGACT00000003511), stat2 (ENSGACG00000000707), stat3 (ENSGACT00000011411), stat4 (ENSGACG00000002684), stat5 (ENSGACG00000015405), stat6 (ENSGACG00000008477); Zebra Finch (*Taeniopygia guttata*) Stat6 (ENSTGUG00000015716); Zebrafish (*Danio rerio*) stat1a (ENSDARG00000006266), stat1b (ENSDART00000059638), stat2 (ENSDART00000050682), stat3 (ENSDART00000022006), stat4 (ENSDART00000105764), stat5.1 (ENSDARG00000019392), stat5.2 (ENSDARG00000055588), stat6 (ENSDART00000059346).

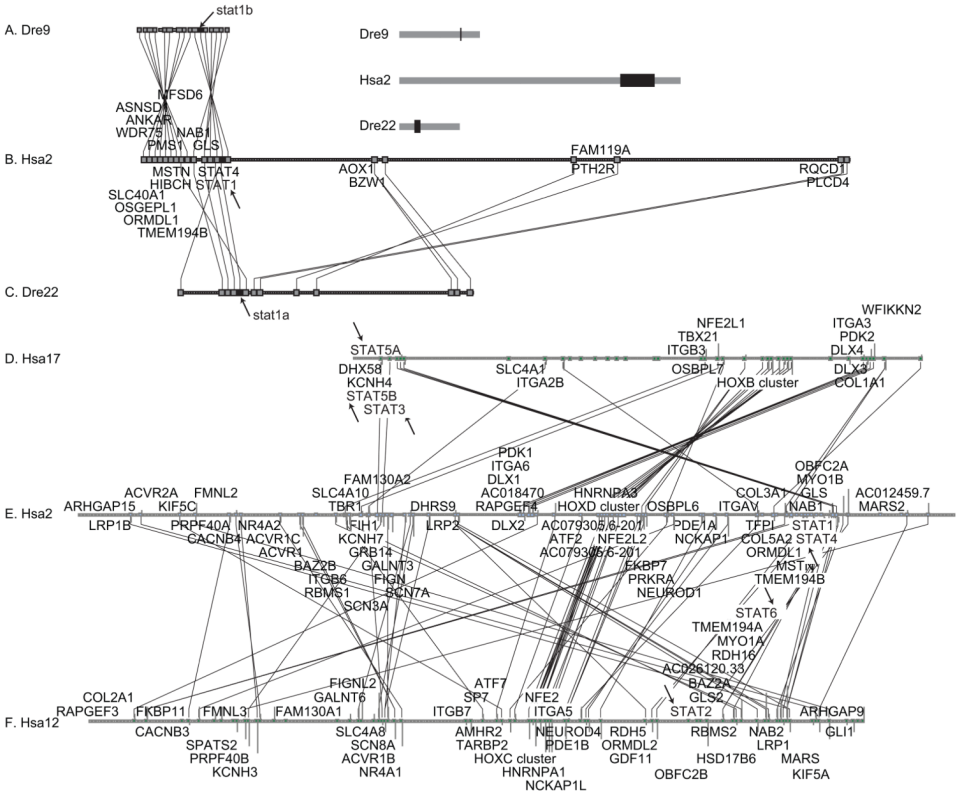

Figure 3.

Conserved syntenies verify the history of the *stat1* gene family. A. Conserved syntenies around zebrafish *stat1b* on zebrafish chromosome Dre9 were searched in the human genome using the Synteny Database (Catchen et al., 2009). B. Extensive conserved syntenies were found around *STAT1* on human chromosome Hsa2. Lines between large boxes connect orthologs; small boxes represent genes without orthologs in the diagramed regions. C. Conserved syntenies around human *STAT1* also appeared around zebrafish *stat1a* on Dre22. Chromosomal regions shown in black rectangles in the insert to the right of part A are blown up in parts A, B, and C. Arrows indicate the positions of *stat* genes. Note that on Hsa2 and Dre9 *STAT1/stat1* and *STAT4/stat4* reside adjacent to each other. Genes (indicated in the order: *HUMAN gene, dre9 gene, dre22 gene*): *STAT4, stat4; STAT1, stat1b, stat1a; GLS, gls, gls; NAB1, NP_001116745.1, si:dkeyp-84a8.1; TMEM194B, B0UYT4; MFSD6, zgc: 92925, si:dkey-188p4.2; HIBCH, hibch; MSTN, mstn, gdf8; PMS1, pms1; ORMDL1, ormdl1; OSGEPL1, osgepl1; ANKAR, ankar; slc40a1, slc40a1; WDR75, wdr75.* The following genes are *HUMAN, dre22gene: RQCD1, rqcd1; PLCD4, plcd4a; PTH2R, si:dkeyp-4h4.1; FAM119A, zgc:110528; FAM119A; AOX1, aox1; BZW1, bzw1a*. D–F. Human *STAT* genes occupy paralogy groups that appear to have originated in the R1 and R2 rounds of genome duplication that preceded the vertebrate radiation. Human paralogs of genes residing in the 20 Mb region of Hsa2 surrounding *STAT1* between 180 and 200 Mb were plotted on the rest of the human chromosomes with gene order according to the location on human chromosome 2 (Hsa2) using the Dotplot feature of the Synteny database (Catchen et al., 2009). Results showed that Hsa2 genes, including *STAT1* and *STAT4*, showed extensive paralogy with Hsa12, which contains *STAT2* and *STAT6*, with Hsa17, which contains *STAT3*, *STAT5A* and *STAT5B* (arrows), and with Hsa7, which lacks any *STAT* genes and is thus omitted from the figure, but has many other paralogs closely linked to *STAT* genes, e.g., potassium channel family H (KCNH2, 7q36.1; KCNH7, 2q24.2; KCNH3 12q13; KCNH4, 17q21.2), the *HOX* clusters (*HOXA4*, 7p15.2; *HOXD4*, 2q31.1;

HOXC4, 12q13.3; *HOXB4*, 17q21.32), erythroid-derived nuclear factor-2 (NFE2L3, 7p15.2; NFE2L2, 2q31; NFE2, 12q13; NFE2L1, 17q21.3), and many other gene families.

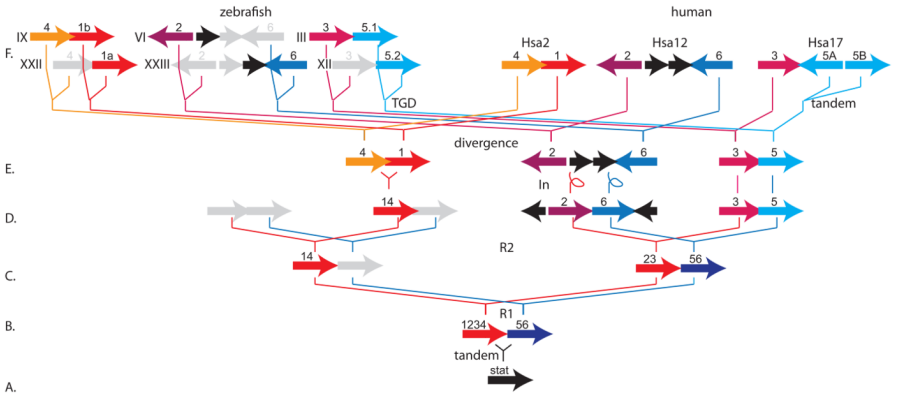

Figure 4.

A model for the origin of vertebrate *STAT* genes. A. The single *STAT* gene in the last common ancestor of all vertebrates. B–E. Sequential steps of genome duplication and gene loss (gray arrows). F. Current arrangements of *STAT* genes in today's zebrafish and human genomes. See text for more explanation. Abbreviations: 1234, the ancestor of *STAT1*, *STAT2*, *STAT3*, and *STAT4*; 14, the ancestor of *STAT1* and *STAT4*; 56, the ancestor of *STAT5* and *STAT6*; divergence, the speciation event that separated the human and zebrafish lineages; In, chromosomal inversions; R1, R2, two sequential rounds of whole genome duplication at the base of vertebrate origins; roman numerals, zebrafish chromosomes; tandem, a tandem duplication event; TGD, teleost genome duplication event.

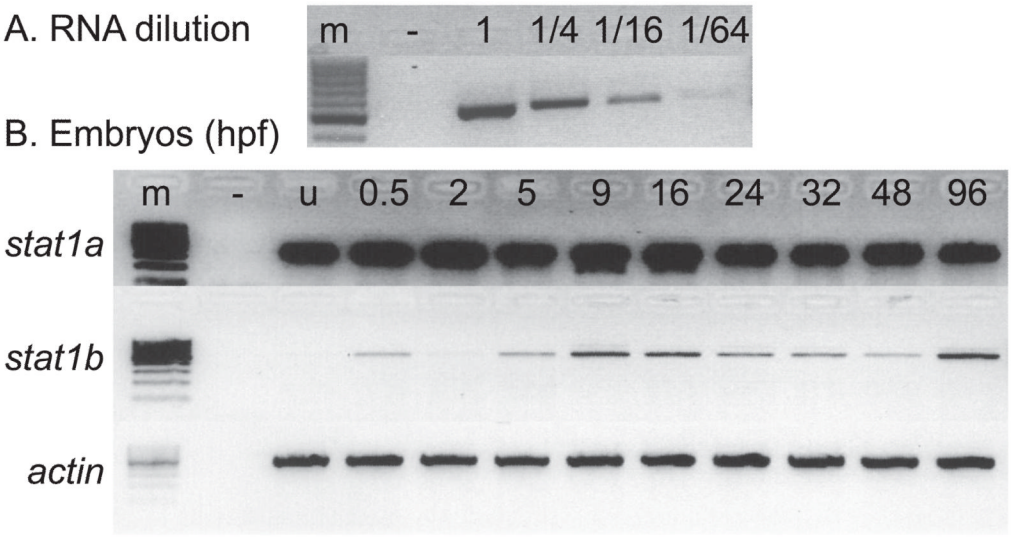

Figure 5.

stat1 gene expression assayed by RT-PCR. A. Calibration series. A gradient of RNA dilutions and 21 amplification cycles with *stat1b* primers verified a semi-quantitative analysis of target mRNAs. B. Detection of *stat1a* and *stat1b* expression using RT-PCR at various stages of development using *beta actin* expression as loading control. RNA samples were extracted from zebrafish embryos at the indicated ages. Abbreviations: –, negative control with no RNA added; u, unfertilized eggs; 0.5, 2, etc., ages at hours post fertilization (hpf).

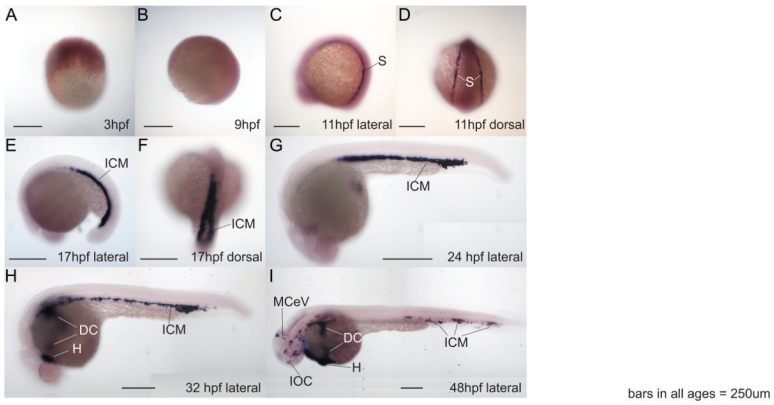

Figure 6.

Whole mount RNA *in situ* hybridization shows specific expression pattern of *stat1b* in zebrafish hematopoietic regions. A, B. 3 hpf and 9 hpf embryos, respectively, did not show specific expression of *stat1b*. C, D. At 11 hpf (2 somites), *stat1b* was expressed in stripes flanking the paraxial mesoderm, shown in lateral and dorsal views, respectively. E, F. At 17 hpf (18 somites), *stat1b* was expressed in the intermediate cell mass, shown in lateral and dorsal views, respectively. G. By 24 hpf, *stat1b* expression stripes had merged centrally. H. At 32 hpf, the *stat1b* expression compartment had spread from the intermediate cell mass to the heart and ducts of Cuvier on the yolk. I. At 48 hpf, the expression of *stat1b* continued in hematopoietic regions and veins. Abbreviations: dc, ducts of Cuvier; h, heart; icm, intermediate cell mass; IOC, inner optic circle; MCeV, middle cerebral vein (Isogai et al., 2001); s, stripes flanking the paraxial mesoderm.

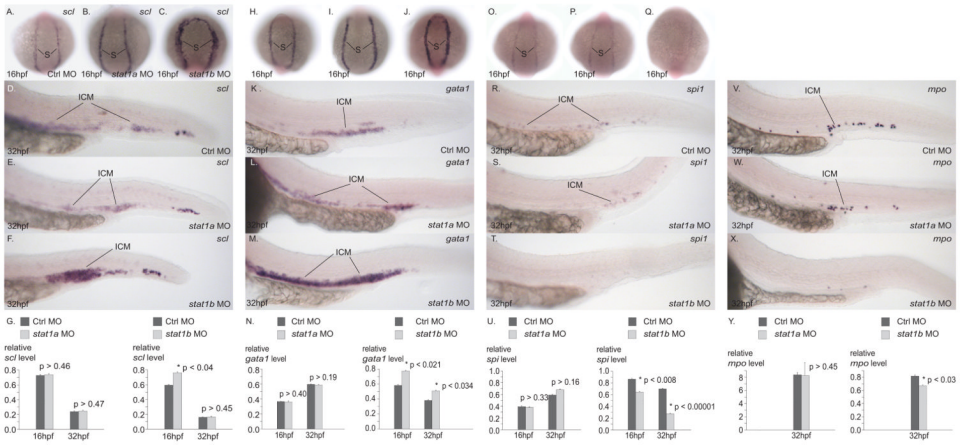

Figure 7.

Gene knockdowns investigate the roles of *stat1a* and *stat1b* in hematopoiesis. In situ hybridization with probes for *scl* (A–G), *gata1* (H–N), *spi1* (O–U), and *mpo* (V–Y) in 16 hpf embryos (A–C, H–J, O–Q) and 32 hpf embryos (D–F, K-M, R–T, V–X) injected with control sequence MO (A, D, H, K, O, R, V), *stat1a* MO (B, E, I, L, W), and *stat1b* MO (C, F, J, M, X). Quantitative PCR experiments (G, N, U, Y). Knockdown of *stat1a* did not alter the expression of the genes tested, but knockdown of *stat1b* led to increased expression of *scl* and *gata1*, markers of HSCs and erythrocytes, and to depressed expression of *spi1* and *mpo*, markers of the myelocyte lineage. These results would be expected if normal *stat1b* activity helped promote a lineage switch from the erythroid to the myeloid lineage.